Margin Failures in Brittle Dome Structures: Relevance to Failure of Dental Crowns

Tarek Qasim,[1] Chris Ford,[1] Mark B. Bush,[1] Xiaozhi Hu,[1] Kenneth A. Malament,[2] Brian R. Lawn[3]

[1] School of Mechanical Engineering, The University of Western Australia, Crawley, Western Australia 6009, Australia

[2] Department of Prosthodontics, Tufts University of Dental Medicine, Boston, Massachusetts 02111

[3] Materials Science and Engineering Laboratory, National Institute of Standards and Technology, Gaithersburg, Maryland 20899-8500

Received 14 November 2005; revised 22 February 2006; accepted 22 February 2006
Published online 13 April 2006 in Wiley InterScience (www.interscience.wiley.com). DOI: 10.1002/jbm.b.30571

Abstract: Margin cracks in loaded brittle dome structures are investigated. Dome structures consisting of glass shells filled with polymer resin, simulating the essential features of brittle crowns on tooth dentin, provide model test specimens. Disk indenters of diminishing elastic modulus are used to apply axisymmetric loading to the apex of the domes. Previous studies using hard indenters have focused on fractures initiating in the near-contact region of such specimens, including radial cracks at the glass undersurface directly below the contact axis. Here, we focus on fractures initiating at the remote support margins. Margin cracks can become dominant when loading forces are distributed over broad contact areas, as in biting on soft matter, here simulated by balsa wood disks. Cracks preinitiated at the dome edges during the specimen preparation propagate under load around the dome side into segmented, semilunar configurations reminiscent of some all-ceramic crown failures. Finite element analysis is used to determine the basic stress states within the dome structures, and to confirm a shift in maximum tensile stress from the near-contact area to the dome sides with more compliant indenters. © 2006 Wiley Periodicals, Inc. J Biomed Mater Res Part B: Appl Biomater 80B: 78–85, 2007

Keywords: all-ceramic crowns; lunar cracks; crown failure; stress analysis

INTRODUCTION

Brittle coatings on polymeric substrates are of interest in relation to a wide range of engineering structures, including biomechanical prostheses.[1] Dental crowns are a special case in point.[2–8] Such structures afford protection for the soft underlayer (dentin) by stress shielding and containment of any cracking within the brittle outer layer (crown). But this tendency to cracking also renders crown structures susceptible to failure in chewing function. There is a need to understand the fundamental cracking modes responsible for such failure, in order that dental practitioners may design structures with longer lifetimes.

Several studies have been reported in the materials literature on potential failure modes in basic crown-like structures subjected to "occlusal" contact loading. Most of these studies have been made on model flat glass/polycarbonate bilayers, in the interest of simplicity.[1,8–13] Glass is the quintessential brittle material, with elastic modulus close to that of tooth enamel and dental porcelain; polycarbonate represents the polymeric dentin support. More recently, these studies have been extended to dome-like polymer-filled glass shells, taking us one step closer to realistic crown geometry.[14–16] Most contact testing has been performed using hard spherical indenters to provide a worst-case occlusal scenario (as well as to preserve the indenter). Several crack types originate in the glass along the contact axis, the most deleterious of which are radial cracks that initiate at the undersurface and run around to the specimen edges.[14–16] Cone cracks which initiate at the top contact surface can penetrate the glass thickness under exacting test conditions, notably cyclic loading in water.[17] Thus, even the most simplistic of simulated crown-like structures are subject to failure from competing fracture modes, each of which may dominate under certain functional conditions.

In this article, we investigate an altogether new mode of fracture in crown-like structures, one that originates at the

Correspondence to: B. R. Lawn (e-mail: brian.lawn@nist.gov)
Contract grant sponsor: Australian Research Council
Contract grant sponsor: National Institute of Dental and Craniofacial Research; contract grant number: PO1 DE10976
Information on product names and suppliers in this article is not to imply endorsement by NIST.

Figure 1. Failure of all-ceramic molar crown, showing semilunar chip from lingual side.

support margins remote from the contact zone. There is some evidence for such a mode in the dental literature, in the form of so-called "semilunar" fractures in which a segment of the crown chips off from one side of the tooth.[4–6,18–20] An example is shown in Figure 1. To investigate the feasibility of such a failure mode, we describe tests on model hemispherical glass shells filled with epoxy resin, similar to specimens used in previous studies but now indented with softer flat disks in order to simulate more closely the effect of intervening medium on chewing loading. Our hypothesis is that such softer indenters will spread the load at the occlusal surface, thereby inhibiting top-surface fracture by shifting tensile stresses around the dome sides toward the margins. Accordingly, use is made of flat-disk indenters of systematically diminishing modulus—from hard metal (steel) to filled polymer (dental composite) to unfilled epoxy resin (pure polymer) to balsa wood (soft food). We will show that first, in switching from metal to filled polymer to epoxy, the reduction in modulus simply increases the loads to initiate and spread radial fractures. However, in the case of ultrasoft balsa wood, the radial mode becomes suppressed, and preexisting cracks at the dome edges begin to extend stably around a section of the dome, ultimately creating a chip resembling the semilunar geometry. Stress analysis using finite element analysis (FEA) will be used to support the experimental observations.

EXPERIMENTAL METHOD

Specimen Fabrication

Curved glass/epoxy bilayer structures were fabricated as previously described,[14,15] but with some specific attention to margin geometry. Glass slides 1 mm thick (D263, Menze-Glaser, Germany) were first heated to 750°C over a metal sphere die of radius $r_s = 6$ mm, forming a plate with hemispherical dimple. The selected heat-treatment temperature enabled shaping of the glass without reduction in thickness; the selected die radius enabled ease of specimen handling in the subsequent finishing stages. After rapid cooling to solidify the shells, a second heat treatment at 550°C was made to eliminate any residual stresses. Hemispherical shells were then prepared by grinding away the base of the glass slides with grade 120 SiC grit paper.

The glass shells were then subjected to controlled sandblast treatments to simulate routine dental finishing procedures. First, the glass undersurfaces were lightly sandblasted with 50 μm particles using a dental sandblast machine (PG Harnish & Reith, Czech Republic), as in the preceding study.[14] This treatment favors the initiation of contact-zone radial cracks. Then the margins were given a second, more severe sandblast treatment with 120 μm particles, so as to shift the balance toward margin fractures. This sandblast treatment simulates the dental practice of edge trimming with diamond burrs, in order to fit the crown snugly onto the tooth. Spurious edge chipping from the severe grinding was apparent in several of the specimens, in some instances leading to premature margin cracks running as much as half way up the dome walls.

One set of specimens was then taken and fitted into molds of the same diameter as the shells, hemispherical protrusion outward.[14] Epoxy resin (R2512, ATL Composites, Australia) was then poured into the mold layer-by-layer, allowing 1 day between layers to ensure curing with minimal shrinkage and bubble formation. Addition of these epoxy layers continued until the shells were fully filled, with additional cylindrical support bases of depth $h = 3$ mm, as in Figure 2.

A second set of shells was epoxy-filled flush with the base diameters (i.e., without the additional cylindrical support) and

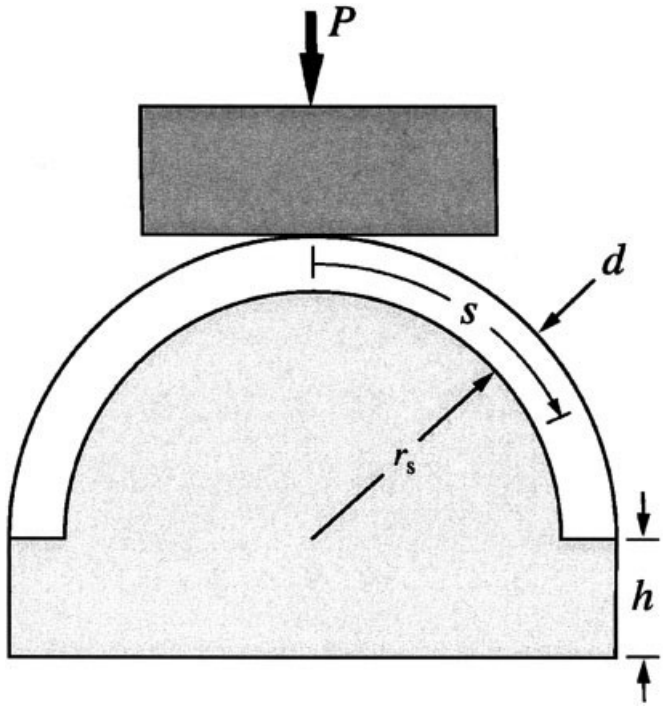

Figure 2. Schematic showing indentation with flat disk at axial load P on crown-like structure consisting of a brittle hemispherical shell of thickness d and inner radius r_s supported by polymeric dentin-like base extending depth h below margin edges.

TABLE I. Materials Properties for Input Into FEA

Material	Young's Modulus (GPa)	Poisson's Ratio
Glass	73	0.21
Steel	220	0.30
Dental composite (Z100)	17	0.33
Epoxy resin	3.4	0.35
Balsa wood	0.05	0.10

then supported at their edges by four equi-spaced steel balls of radius 8 mm. This was to exaggerate the effect of concentrated loads at the base, as might be experienced by crowns with undulating margins (e.g. Figure 1).

Failure Testing

The filled domes were loaded along their symmetry axes with various disk indenters of fixed diameter 10 mm (Figure 2): metal (silver steel, Bohler Steel, Canning Vale, Western Australia), dental composite (Z100, 3M Dental Products, St Paul, Minn), epoxy resin (same as shell filler) of thickness 3 mm; and balsa wood of thickness 10 mm. These materials were selected in order to cover a range of elastic modulus (Table I). The ultrasoft balsa wood, although possessing a complex, anisotropic cellular structure, can be considered representative of typical fibrous soft food experienced in everyday chewing.

Single-cycle tests were made at $\sim$10 N s^{-1} up to loads P = 2000 N in air with the indenter mounted into the cross beam of a mechanical testing machine (Instron 4301, Instron, Canton, MA). A video camera (TRV33E, Sony, Japan) was used to monitor the specimen, with diffuse lighting behind the specimen to enhance visualization of the cracks. Where possible, the crack evolution was observed *in situ* during testing. However, with softer indenters this was not always easy, because of engulfment of the top surface regions. In these latter cases, crack progress was observed sequentially after periodic load–unload steps. No indication of any delamination of the epoxy filler from the glass walls was evident in any of these tests.

Finite Element Analysis

A similar algorithm to that in earlier studies was used to determine the stress distributions,[14,16,21] but now with the hemispherical brittle shells built into the cylindrical polymeric support base, Figure 2. In accordance with experiment, the following parameters were input into the algorithm: glass dome, thickness d = 1 mm and internal radius r_s = 6 mm; epoxy resin support, radius (r_s + d) = 7 mm and depth h = 3 mm; flat disk indenters, 10 mm diameter and prescribed thickness 3 mm (metal, dental composite and epoxy resin) or 10 mm (balsa wood). The deformation was assumed to be elastic everywhere over the load ranges covered. Young's modulus and Poisson's ratios used in the calculations are listed in Table I.

The disk indenters were loaded stepwise over the experimental range, normally and axisymmetrically along the dome axis. Meshes were systematically refined, particularly in the critical glass undersurface region, until the solutions attained convergence. Out-of-plane hoop tensile stress and in-plane maximum compressive stress distributions within the dome structures were calculated at each load step.

RESULTS

Experiments

Crack patterns are shown in Figure 3 for the three harder indenters (i.e., excluding balsa wood), i.e., (a) metal, (b) filled polymer and (c) epoxy, at a common load P = 1000 N. These

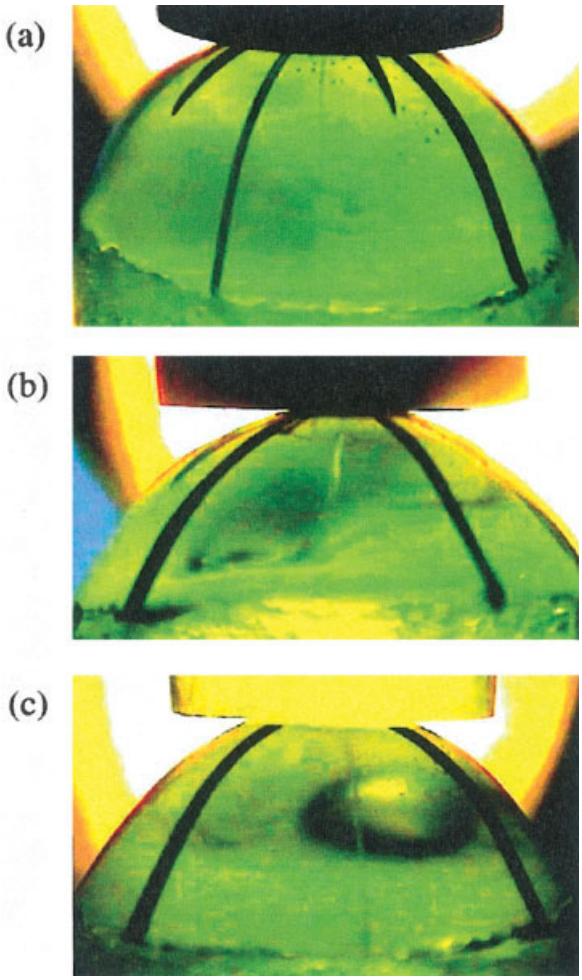

Figure 3. Contact fracture of epoxy-filled glass domes of inner radius r_s = 6 mm and thickness d = 1 mm on epoxy support base extending h = 3 mm below dome margins, indented at load P = 1000 N with disks of thickness 3 mm: (a) steel, (b) dental composite, and (c) epoxy. Showing failure from radial cracks. Note diminishing intensity of radial cracking with diminishing indenter modulus (left to right). (Balsa wood indenters produce no radial cracks up to 2000 N.) [Color figure can be viewed in the online issue, which is available at www.interscience.wiley.com.]

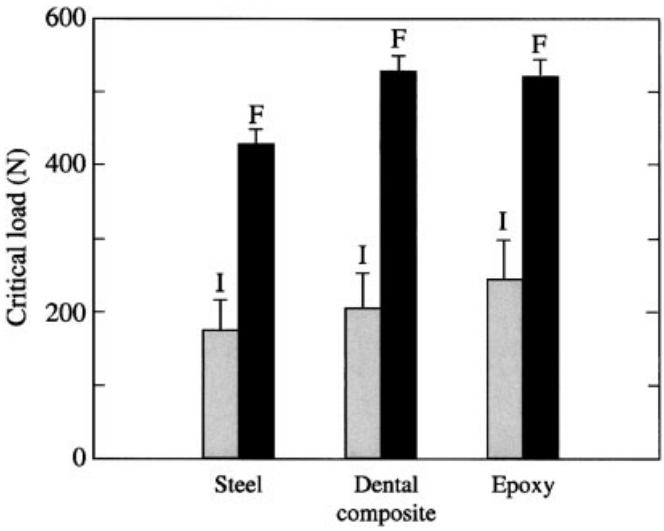

Figure 4. Histogram showing critical loads to initiate radial cracks (I) and to propagate these same cracks to failure at the edges of glass domes (F), for same indenters represented in Figure 3.

all reveal dominant radial cracks initiating from the near-contact zone and propagating to the dome edges. The radial cracks have much the same form as those produced with hard spherical indenters, as described in the preceding study.[14] However, with the more compliant indenters the radial crack pop-in was not quite so abrupt—less multiple radial cracking and spurious cone cracking occurred, and it took a little longer for the radials to grow to the edges of the domes. These observations are consistent with some diminution in the contact stress intensity with diminishing indenter modulus. Figure 4 quantifies these observations by plotting critical loads to initiate (I) and to propagate radial cracks to failure (F) at the specimen edges, with standard deviation bounds for a minimum of four tests in each case (error bars). Note the small increase in critical loads as the material modulus diminishes from left to right. In tests with balsa indenters, no radials could be formed at all beneath the contact area up to loads of 2000 N.

Figure 5 shows a dome after indentation with a balsa wood disk. The sequence has been photographed intermittently between load increments: (a) $P = 0$, (b) 500 N, (c) 1000 N, (d) 2000 N. [The indenter is photographed in place in Figure 5(a) only.] This specimen contains preexisting margin cracks from the specimen preparation [Figure 5(a)]. Note the absence of top-surface radial cracks over the load range. The margin cracks grow incrementally upward without deviation at 500 N [Figure 5(b)]. Propagation continues further upward at 1000 N, but the cracks now link up laterally to form a disjointed but closed failure pattern [Figure 5(c)]. The cracking continues to intensify at 2000 N, running around rather than over the top of the dome, with the linked crack segment still in place [Figure 5(d)]. It is not difficult to imagine the closed segment delaminating to form a dislodged chip with further overload.[14]

Another example of the evolution of preexisting margin cracks is given in Figure 6, for loading with a balsa wood indenter at $P = 500$ N. Two margin cracks are inclined to the median plane of the dome. In this example, the cracks have propagated continuously around the dome face into a smooth U-turn. Continued loading caused these cracks to propagate further down back toward the margin into a near-parabolic configuration, somewhat closer to the smooth semilunar fracture geometry seen in Figure 1.

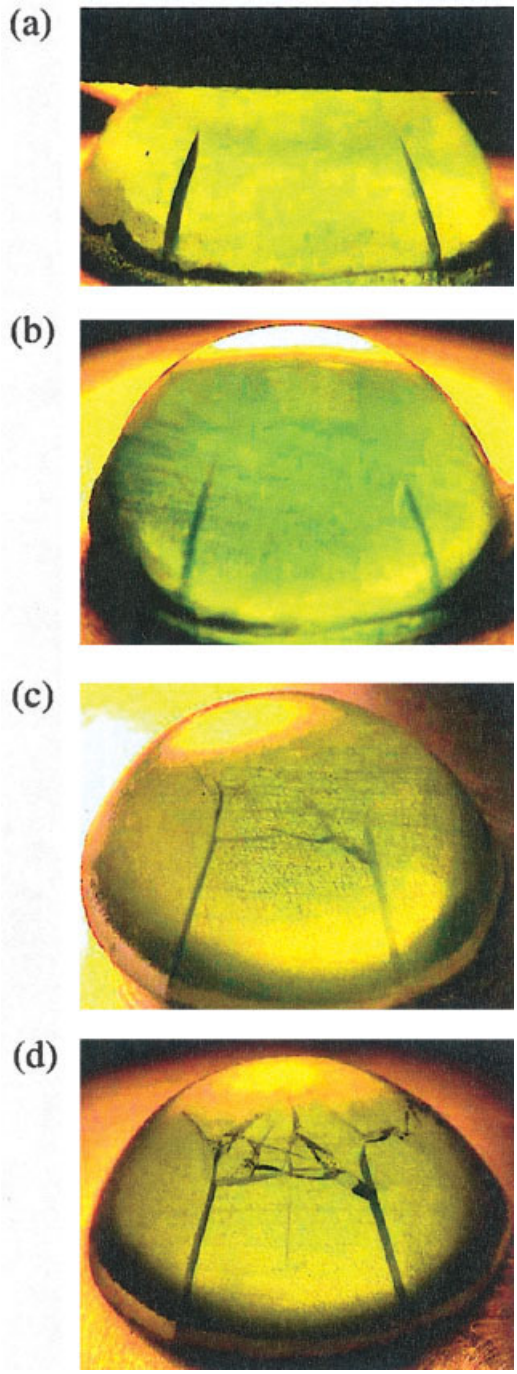

Figure 5. Evolution of preexisting margin cracks from grinding preparation in epoxy-filled glass dome, dimensions $r_s = 6$ mm, $d = 1$ mm, $h = 3$ mm. Balsa wood indenter at loads (a) $P = 0$, (b) 500 N, (c) 1000 N, and (d) 2000 N. Note linkage of adjacent margin cracks in (c) and intensification in (d). [Color figure can be viewed in the online issue, which is available at www.interscience.wiley.com.]

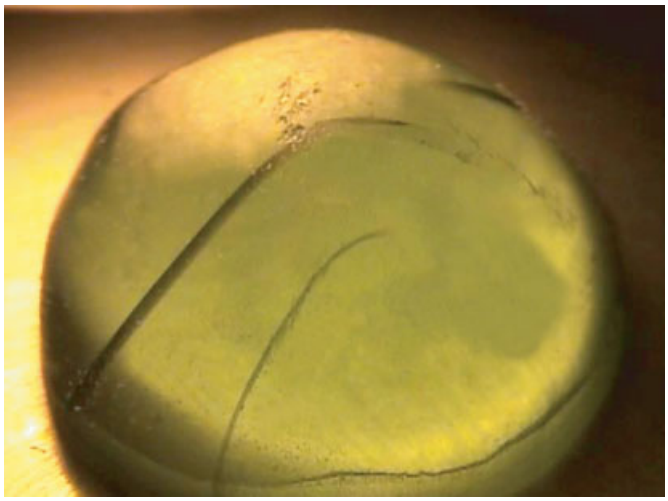

Figure 6. Growth of preexisting margin crack from edge grinding flaws in epoxy-filled glass dome, r_s = 6 mm, d = 1 mm, h = 3 mm. Balsa wood indenter at load P = 500 N. Crack is shown bending into a U-turn to form more continuous lunar-like fracture. [Color figure can be viewed in the online issue, which is available at www.interscience.wiley.com.]

In no case did specimens on a uniform cylindrical support base but without preexisting margin cracks fail by lunar fracture over the load range up to 2000 N, regardless of indenter material. (In some instances, some secondary small-scale marginal chipping occurred during loading.) However, specimens with concentrated four-ball support provided an exception. Figure 7 is one such example, again with balsa indenter at P = 500 N. Margin cracks have popped in abruptly from the vicinity of one of the sphere supports to produce a substantial side-surface chip fracture. This example serves to show that side-wall failures are entirely possible in extreme margin geometries.

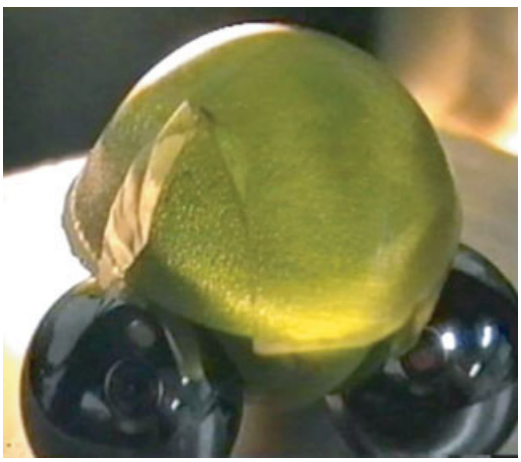

Figure 7. Fracture of epoxy-filled glass dome, r_s = 6 mm, d = 1 mm, h = 3 mm. Balsa wood indenter at load P = 500 N, supported on four steel balls. This specimen contained no preexisting margin cracks, and spontaneously developed the chip fracture shown. [Color figure can be viewed in the online issue, which is available at www.interscience.wiley.com.]

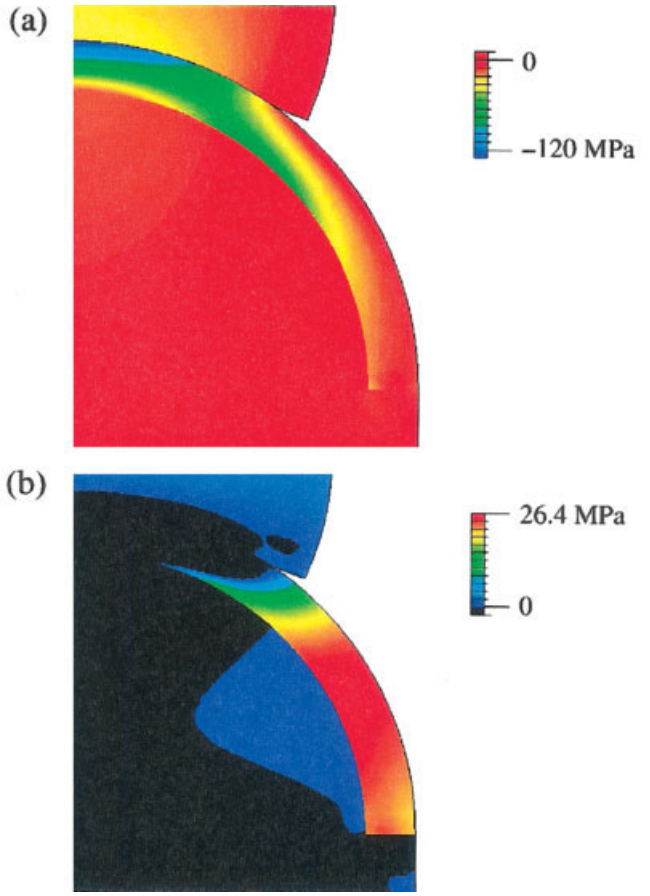

Figure 8. Finite element analysis of stress distributions in epoxy-filled glass domes of thickness d = 1 mm on epoxy support base extending h = 3 mm below dome margins, indented at load P = 1000 N with balsa wood disk of thickness 10 mm: (a) in-plane principal compressive stress, color intervals 10 MPa; (b) out-of-plane hoop tensile stress, color intervals 2.2 MPa (compressive stresses black). Stresses are larger on the inner glass surface. Note maximum tensile stress about two thirds of the circumference around the dome face.

FEA Stress Analysis

Stress contours of maximum in-plane compression and out-of-plane hoop tension are shown in Figure 8 for a glass/epoxy dome structure loaded with balsa wood indenter at P = 1000 N. The compression contours [Figure 8(a)] are highest beneath the spread-out contact, as expected. Some of the compression stress has been transmitted to the epoxy filler, but most resides within the stiff shell. Outside the contact the contours tend to parallelism with the sphere surface, indicating an effective transfer of load to the shell margins. The tensile contours [Figure 8(b)], on the other hand, are concentrated outside the contact. The absence of any tension within the contact zone explains the absence of top-surface radial cracking in tests with balsa indenters. The tensile maximum (≈26 MPa at the load represented) is thereby shifted toward the margins, approximately two thirds around the inner shoulder. The magnitude of both stress components outside the contact tend to be higher on the inner than outer shell walls.

Figure 9 plots the hoop tensile stress on the inner glass surface as a function of coordinate s (Figure 2) for the

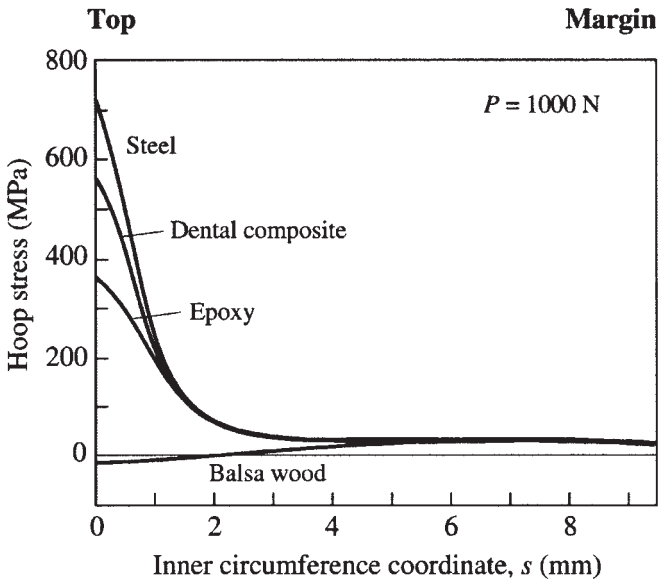

Figure 9. Distribution of hoop tensile stress around epoxy-filled glass dome inner surface as function of coordinate *s* (Figure 2), for indentation at load $P = 1000$ N with steel, dental composite, epoxy and balsa wood disks. Note sensitivity of stresses to indenter material at axial contact location $s = 0$, insensitivity at margin location $s = 9.4$ mm. Note especially curve for balsa with tensile maximum at $s \sim 6$ mm.

four-test indenters, again at fixed load $P = 1000$ N. In the near-field contact region ($s = 0$), i.e., where the radial cracks form, the tensile stresses are significantly lower for the more compliant indenters. In the special case of balsa wood, the maximum principal stress is actually negative in this region (cf. Figure 8), again highlighting the role of indenter elastic modulus. In the far-field margin region ($s = 9.4$ mm), i.e., where lunar cracks originate, the tensile stresses are virtually the same for all indenters. Note once more that the curve for balsa has its maximum about two thirds around the dome (again, cf. Figure 8). Beyond this maximum, the stress falloff is slow, so that the hoop stress at the margins is still significant. The diminution of crack-path tensile stress levels with decreasing indenter modulus would explain the systematic shift to higher loads needed to initiate and propagate radial cracks alluded to earlier (Figure 4). Predicted critical initiation loads, evaluated from the FEA analysis by equating the maximum hoop tension with a nominal strength 142 MPa for our abraded glass undersurfaces (chosen to match strengths of like-abraded flat bilayers) fall within the error bounds of the experimental values, Table II.

A more detailed indication of hoop stress evolution at the inner glass surface during loading with soft balsa wood is shown in Figure 10, for indentation at 100 N intervals. At low loads, these stresses are maximum tensile directly below the indenter, where radial cracks form ($s = 0$). At higher loads, the stresses at this axial location diminish and ultimately become compressive as the contact radius expands relative to the plate thickness and engulfs the top surface. This engulfment pushes the maximum tensile stress outward and onto the

TABLE II. Comparison of Experimental and FEA Determinations of Critical Loads to Initiate Radial Cracks in 1 mm Glass on Epoxy Using Different Indenters

Indenter Material	Experimental (N)	FEA (N)
Steel	175 ± 40	171
Dental composite (Z100)	205 ± 47	188
Epoxy resin	243 ± 54	241

dome shoulders.[22] The hoop stresses reach a maximum value about two thirds around the dome walls. Note again the slow stress falloff beyond the maximum. The stresses at the margin ($s = 9.4$ mm) are always tensile and increase more or less linearly with load.

DISCUSSION

This work has demonstrated how ultracompliant indenters, simulating chewing with food, can change the basic mode of fracture in brittle crown-like structures. Most prior studies have been conducted on flat bilayer specimens or (more recently) on dome structures with uniform support at margins (Figure 2), using hard spherical indenters.[7,8,14] In those earlier studies the confined contact between hard indenter and brittle surface favored a flexural mode of fracture, leading to dominant radial cracks or some other form of near-contact fracture (e.g., cone cracking). In the present study, on filled glass domes, transition to an ultrasoft disk indenter, representative of food bolus, induces a marked change in fracture

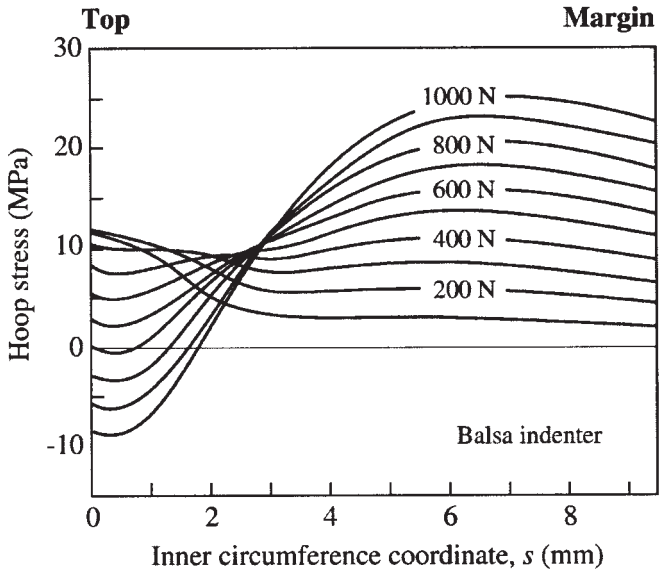

Figure 10. Distribution of hoop tensile stress around epoxy-filled glass dome inner surface as function of coordinate *s* (Figure 2), balsa wood disk indenter at increasing loads *P*.

response. The softer contact spreads the load, shifting the tensile stresses around the side walls toward the margins, suppressing top-surface radial cracking and thereby favoring edge failures. In the case of axial loading studied here, such failures develop from preexisting margin cracks as a result of the dome edge-grinding and sandblasting process during preparation. These cracks evolve during loading into curved cracks with ultimate chip formation, resembling so-called semilunar crown fractures. Chipping may occur by linking up of adjacent margin cracks or by smooth propagation of an initially inclined margin crack along a near-parabolic, sidewall path. Recall from Figures 8–10 that the tensile stresses in such configurations tend to maxima on the shoulder of the dome, typically about two thirds around the dome face, so that once margin cracks have popped in, they become easier to propagate in this region.

It is important to reiterate that the demonstrated semilunar fracture geometries realized in Figures 5 and 6 required the preexistence of margin cracks from preceding specimen sandblast preparation. We saw no evidence of such semilunar fractures in specimens without such preexisting cracks, up to loads of 2000 N. However, our tests were conducted under relatively benign conditions: (i) the domes were prepared with a level base, whereas real crowns have undulating margins which could concentrate stresses at focal support points and promote inclined fractures (e.g., Figure 6). The ease of fracture in specimens on ball supports (Figure 7) demonstrates this clearly. (ii) The domes had walls of uniform thickness (1 mm) with 90° shoulders. Such a configuration is not recommended for real all-ceramic crowns. In actual dental practice, chamfered or rounded shoulders are used to avoid edge stress concentrations. (iii) The tests were run in laboratory air, whereas dental crowns operate in aqueous environment. It is well documented that water can accelerate crack initiation from flaws in brittle materials. (iv) We have run only single-cycle tests—cyclic loading can typically diminish critical initiation loads by more that a factor of 2 over a year or so.[23,24] (v) The tests have been restricted to axial loading—off-axis loading can substantially increase stresses in margin regions, partly by decreasing the distance between contact and margin and partly by stress redistribution.[15] (vi) Our tests have been run only on specimens with single brittle layers, whereas all-ceramic crowns usually consist of double (veneer/core) brittle layers. Stresses in the latter configurations will be transferred preferentially into the stiffer (core) layer,[25] thereby concentrating the stresses even more strongly at the inner margins. (vii) We have used just one material, balsa wood, as our representative "food bolus". Although in reality this material is anistropic and nonlinear in its stress–strain response, we have taken an averaged modulus and assumed linear elastic behavior throughout. Some additional calculations incorporating nonlinear behavior suggest that the contact area may be even larger than shown in Figure 8, with more exaggerated shift in tensile stress toward the margins.

All these effects are expected to lower the critical loads for initiation of margin fracture and for propagation of these cracks into semilunar configurations. We will explore some of them in later studies.

ACKNOWLEDGMENTS

Discussions with Yu Zhang, E. Dianne Rekow and Van P. Thompson at New York University, and Sanjit Bhowmick and Ilja Hermann at NIST, are gratefully acknowledged.

REFERENCES

1. Lawn BR, Deng Y, Miranda P, Pajares A, Chai H, Kim DK. Overview: Damage in brittle layer structures from concentrated loads. J Mater Res 2002;17:3019–3036.
2. Kelly JR. Ceramics in restorative and prosthetic dentistry. Annu Rev Mater Sci 1997;27:443–468.
3. Kelly JR. Clinically relevant approach to failure testing of all-ceramic restorations. J Prosthet Dent 1999;81:652–661.
4. Malament KA, Socransky SS. Survival of Dicor glass–ceramic dental restorations over 14 years. I. Survival of Dicor complete coverage restorations and effect of internal surface acid etching, tooth position, gender and age. J Prosthet Dent 1999;81:23–32.
5. Malament KA, Socransky SS. Survival of Dicor glass–ceramic dental restorations over 14 years. II. Effect of thickness of Dicor material and design of tooth preparation. J Prosthet Dent 1999; 81:662–667.
6. Malament KA, Socransky SS. Survival of Dicor glass–ceramic dental restorations over 16 years. III. Effect of luting agent and tooth or tooth-substitute core structure. J Prosthet Dent 2001; 86:511–519.
7. Lawn BR, Deng Y, Thompson VP. Use of contact testing in the characterization and design of all-ceramic crown-like layer structures: A review. J Prosthet Dent 2001;86:495–510.
8. Lawn BR, Pajares A, Zhang Y, Deng Y, Polack M, Lloyd IK, Rekow ED, Thompson VP. Materials design in the performance of all-ceramic crowns. Biomaterials 2004;25:2885–2892.
9. Jung YG, Wuttiphan S, Peterson IM, Lawn BR. Damage modes in dental layer structures. J Dent Res 1999;78:887–897.
10. Lawn BR, Lee KS, Chai H, Pajares A, Kim DK, Wuttiphan S, Peterson IM, Hu X. Damage-resistant brittle coatings. Adv Eng Mater 2000;2:745–748.
11. Lawn BR. Ceramic-based layer structures for biomechanical applications. Curr Opin Solid State Mater Sci 2002;6:229–235.
12. Deng Y, Lawn BR, Lloyd IK. Characterization of damage modes in dental ceramic bilayer structures. J Biomed Mater Res B 2002;63:137–145.
13. Shrotriya P, Wang R, Katsube N, Seghi R, Soboyejo WO. Contact damage in model dental multilayers: An investigation of the influence of indenter size. J Mater Sci: Mater Med 2003;14:17–26.
14. Qasim T, Bush MB, Hu X, Lawn BR. Contact damage in brittle coating layers: Influence of surface curvature. J Biomed Mater Res B 2005;73:179–185.
15. Qasim T, Ford C, Bush MB, Hu X, Lawn BR. Effect of off-axis concentrated loading on failure of curved brittle layer structures. J Biomed Mater Res B 2006;76:334–339.
16. Qasim T, Bush MB, Hu X. The influence of complex surface geometry on contact damage in curved brittle coatings. Int J Mech Sciences 2006;48:244–248.
17. Zhang Y, Kwang J-K, Lawn BR. Deep penetrating conical cracks in brittle layers from hydraulic cyclic contact. J Biomed Mater Res B 2005;73:186–193.

18. McLean JW. The Science and Art of Dental Ceramics, Vol. 1: The Nature of Dental Ceramics and Their Clinical Use. Chicago: Quintessence; 1979, pp 39–40.
19. Malament KA, Grossman DG. The cast glass–ceramic restoration. J Prosthet Dent 1987;57:674–683.
20. Thompson JY, Anusavice KJ, Naman A, Morris HF. Fracture surface characterization of clinically failed all-ceramic crowns. J Dent Res 1994;73:1824–1832.
21. Ford C, Bush MB, Hu XZ, Zhao H. A numerical study of fracture modes in contact damage in porcelain/Pd-alloy bilayers. Mater Sci Eng A 2004;364:202–206.
22. Chai H, Lawn BR. Fracture mode transitions in brittle coating layers on compliant substrates as a function of thickness. J Mater Res 2004;19:1752–1761.
23. Zhang Y, Pajares A, Lawn BR. Fatigue and damage tolerance of Y-TZP ceramics in layered biomechanical systems. J Biomed Mater Res B 2005;71:166–171.
24. Zhang Y, Lawn BR. Fatigue sensitivity of Y-TZP to microscale sharp-contact flaws. J Biomed Mater Res B 2005;72:388–392.
25. Miranda P, Pajares A, Guiberteau F, Cumbrera FL, Lawn BR. Contact fracture of brittle bilayer coatings on soft substrates. J Mater Res 2001;16:115–126.